Palomar adaptive optics project: status and performance

M. Troy[a], R. Dekany, G. Brack[a], F. Shi[a], B. Oppenheimer[b], T. Trinh[a], E. Bloemhof[c], T. Hayward[d*], B. Brandl[d] , and F. Dekens[a]

[a]Jet Propulsion Laboratory, California Institute of Technology, Pasadena, CA, USA 91109

[b]Astronomy Dept., University of California Berkeley, CA, USA 94720

[c] Palomar Observatory, California Institute of Technology, Pasadena, CA, USA 91125

[d]Astronomy Dept., Cornell University Ithaca, NY, USA 14853

ABSTRACT

We describe the current status of the Palomar 200 inch adaptive optics system, which in December of 1998 achieved its first high order (241 actuators) lock on a natural guide star. Shared risk observing using this facility instrument started in August of 1999, guiding on stars as faint as 13th magnitude. In the K band (2.2 μm) the system has achieved Strehl ratios as high as 50% in the presence of 1.6 arcsecond seeing (0.5 μm). An analysis of the error budget is used to show which sub-systems are limiting the performance of the AO system. Brief discussions of near-term plans and lessons learned are also presented.

Keywords: Adaptive optics, telescopes, instrumentation

1. INTRODUCTION

The Palomar Adaptive Optics system (PALAO) is a facility AO system for use at the f/16 Cassegrain focus of the Palomar 200" Hale telescope. The instrument was built and designed by the Jet Propulsion Laboratory, under the project lead of Rich Dekany. In March of 1998, PALAO achieved its first tip/tilt lock on a natural guide star.[1] About one year latter the system achieved it's first high order lock again on a natural guide star. In August of 1999 the system started shared risk observing supporting 9 groups of observers over 10 nights of observing in five months. In May of 2000 PALAO will become a standard Palomar facility instrument available for use by any observer. The system routinely achieves Strehls of 50% (in K) on guide stars brighter then 10th magnitude in the presence of 1 to 1.5 arcsecond seeing (0.5 μm) with estimated wind velocities on the order of 10 m/s.

The PALAO system has been previously described in Dekany, et al.[1,2] For reference we include a brief description of the optical path. Figure 1 shows a combination ray-trace and AutoCAD drawing, as seen from above, as if looking through the optical bench when mounted at Cassegrain. The light from the secondary mirror passes beyond the Cassegrain focus through the optical bench and is then diverted into the plane by a 45 degree fold mirror (FM1), collimated by an off-axis parabolic mirror (OAP1), tilted by the tip/tilt mirror (FSM), corrected by the deformable mirror (DM), reflected off a flat mirror (FM2), and then reimaged by a second off-axis parabolic mirror (OAP2). The IR light passes through the dichroic and is folded by FM3 to the science camera, while the visible light reflects off the dichroic and second star selection mirror before encountering a reflective spot at the relay focus that serves as a field stop for the wavefront sensors (WFS). Light striking this spots is collimated within the WFS, subdivided by the lenslet array and then reimaged onto the WFS camera. Light missing the field stop is reimaged onto the acquisition camera (ACQ).

2. ON-AXIS BRIGHT GUIDE STAR PERFORMANCE

The performance of an AO system can be characterized in terms of the mean-squared wavefront error (σ^2) is a sum of individual error terms, σ_i^2. This addition of the error terms in quadrature assumes that the individual error terms, σ_i^2 are independent. If the individual error terms are not independent then the total error will be overestimated and the system performance underestimated. A useful metric in quantifying an AO system performance is the Strehl ratio, which is the ratio of the measured peak intensity in the image plane over the peak intensity of a perfect wavefront

*Currently with Gemini Observatory, Hilo, HI 96720

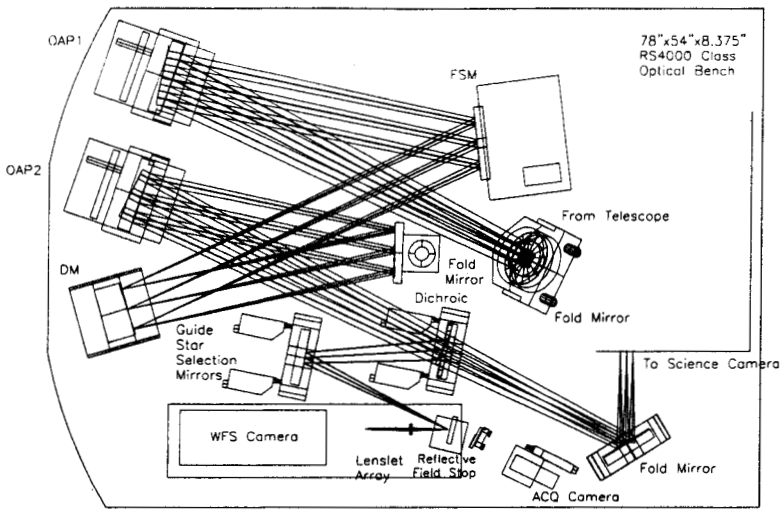

Figure 1. A combination Zemax ray-trace and AutoCAD drawing of PALAO as seen from above, as if looking through the optical bench when mounted at Cassegrain.

propagated through the telescope. When the wavefront errors are less then $\frac{\lambda}{4\pi}$ the Strehl ration can be estimated by the Marechal approximation[3] $S \approx e^{-\sigma^2}$. We describe the performance of a natural guide star adaptive optics system is a sum of error terms:

$$\sigma^2_{BGS} = \sigma^2_{TD} + \sigma^2_{RT} + \sigma^2_{AF} + \sigma^2_{TF} + \sigma^2_{CAL} \tag{1}$$

Where σ^2_{BGS} is the total performance on an on-axis bright guide star, σ^2_{TD} is the time-delay error, σ^2_{RT} is from residual tip/tilt errors, σ^2_{AF} is from fitting the atmosphere to the DM actuator spacing, σ^2_{TF} is from fitting the telescope to the DM actuator spacing and σ^2_{CAL} is the calibration error

While these are not the only error terms for an on-axis "bright" guide star on axis, they are the dominant error terms for the PALAO system. In the remainder of this section we discus the theoretical values of each of the above terms and were possible compare these values to values obtained from operating the system while observing. We conclude this section by bringing all the error terms together to get an estimate of the PALAO system performance and comparing these values to the system performance as measured by PHARO images.

The data used for the analysis was collected on September 30th, 1999 with the system locked on a V=6.6 magnitude guide star (SAO 68125) near the zenith with the WFS running at 500Hz and recording telemetry data at 100Hz. The telemetry data consisted of centroid positions, tip tilt mirror positions and residuals, and DM positions and residuals. Data was collected with both the DM and tip/tilt loops open, just the tip/tilt loop closed, and both the tip/tilt and DM loops closed.

The atmospheric seeing can be measured from the open loop centroid telemetry and the following equation[4]:

$$r_0 = d_s \left[0.4488 \left(\frac{\lambda}{2\pi}\right)^2 \left(\frac{4}{d_s}\right)^2 \left(\frac{1}{\sigma^2_\theta}\right) \right]^{\frac{3}{5}} \tag{2}$$

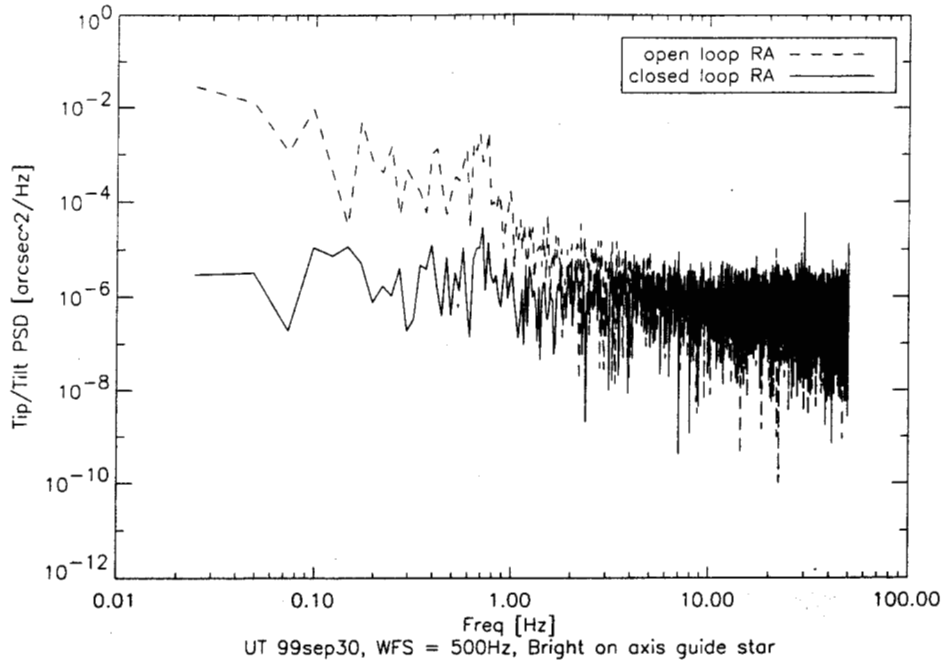

Figure 2. Plot of the PSD of the open and closed loop tilt in right ascension. The open loop residuals are a measure of the atmospheric tilt errors. The servo bandwidth is about 5Hz.

where σ_θ^2 is the mean-square centroid motion over a subapeture of diameter d_s. r_0 is the the Fried parameter calculated at a wavelength of λ which is not necessarily the wavelength where the centroid motion was measured. Using the above equation and an open loop data set 61 sec. long (collected with the parameters previously mentioned) r_0 was calculated to be 10 cm at 0.5 μm. This calculation was carried out for each of the approximately 241 WFS subapetures (d_s = 31.2 cm) then r_0 averaged over all the measurements. This provides a result (for the most part) independent of the outer scale of turbulence. The wind velocity was about 5 m/s (estimated from the break frequency of the open loop tip/tilt PSDs, Figures 2 and 3).

2.1. Time-delay σ_{TD}^2

The mean-square phase error resulting from the servo control loop and time-delay is[5]:

$$\sigma_{TD}^2 = k\left(\frac{f_G}{f_S}\right)^{5/3} \tag{3}$$

where f_S is the servo bandwidth of the system and k ranges from 1 for a simple RC network, to 0.191 for a perfect cutoff filter at frequency f_S. The PALAO servo algorithm is more like an RC filter, so we use a value of 1 for k. f_G is the Greenwood frequency, which may be approximated by:

$$f_G = 0.427\frac{v}{r_0} \tag{4}$$

where the atmosphere is assumed to have a single turbulent layer with wind velocity v.

The closed loop DM residual errors provide an independent estimate of σ_{TD}^2. For a given frame of WFS data the closed loop centroids values are taken and then multiplied by the reconstructor to get the error of each DM actuator. The RMS wavefront error is then approximately two times the RMS of these actuators values. The resulting σ_{TD} value is 68 nm. Figure 4 is a PSD plot of the open and closed loop DM residuals. From the plot the estimated value for f_S is 15 Hz. Using f_S = 15 Hz, v=5 m/s, and $r_0(0.5\ \mu m)$ Eq. 3 predicts σ_{TD} = 107 nm.

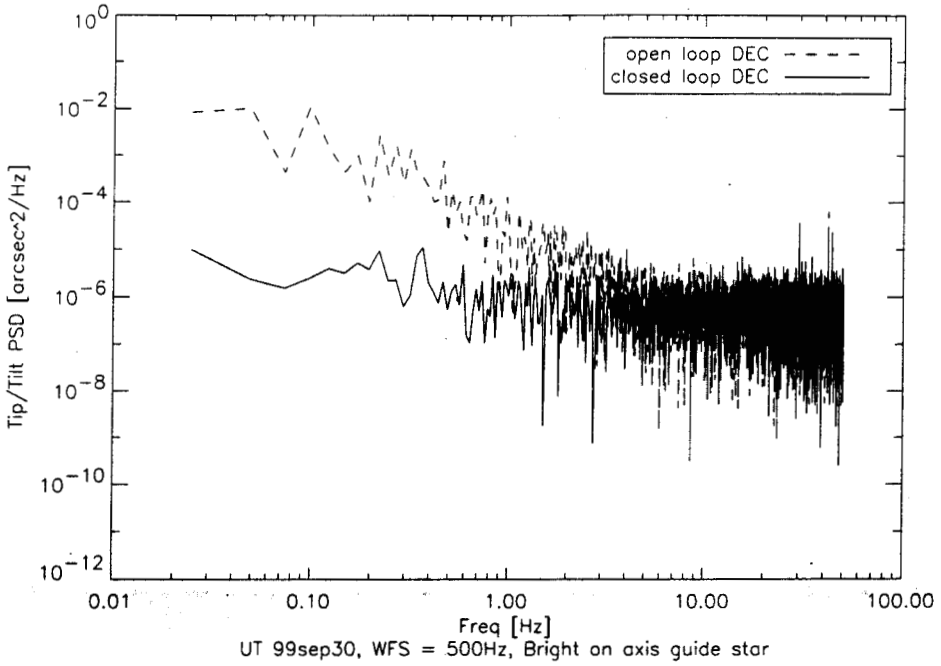

Figure 3. Plot of the PSD of the open and closed loop tilt in declination. The open loop residuals are a measure of the atmospheric tilt errors. The servo bandwidth is about 5Hz.

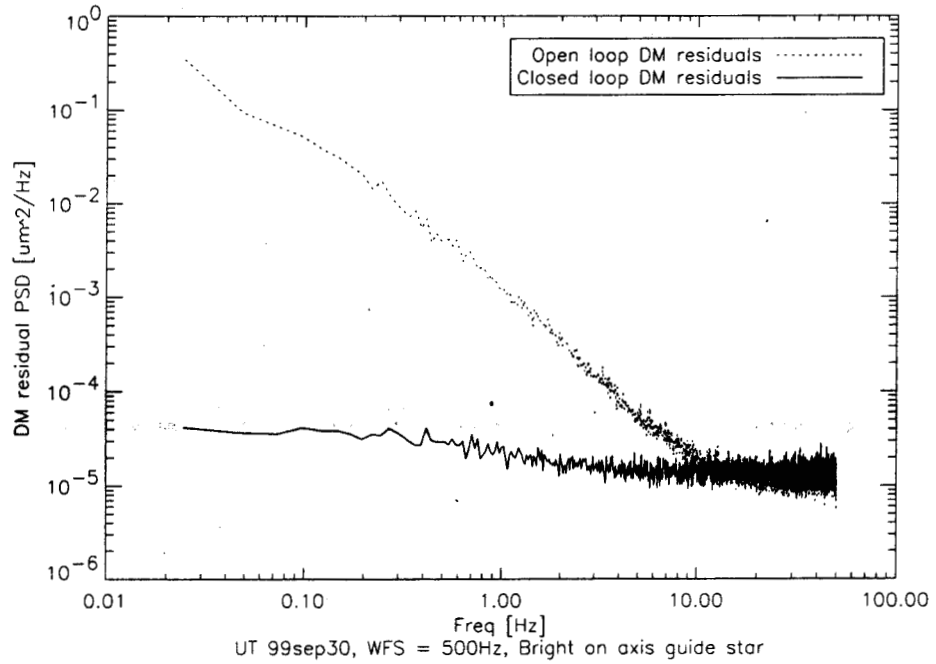

Figure 4. Plot of the power spectral density (PSD) of the open and closed loop DM residuals. The open loop DM residuals are a measure of the atmospheric phase errors. The PSD's were calculated for each actuator and then averaged. The servo bandwidth is about 15Hz.

2.2. Residual Tip/Tilt Error σ^2_{RT}

The residual tip/tilt error from the finite-bandwidth of the AO tip/tilt correction is given by[6]:

$$\sigma_{RT} = \left(\frac{f_T}{f_{3dB}}\right)^{1/6} \left(\frac{\lambda_T}{D}\right) \tag{5}$$

Where f_T is the fundamental tilt tracking frequency. Assuming one layer of atmospheric turbulence at an altitude h and a zenith angle of zero, the tracking frequency can be approximated by[7]:

$$f_T \approx 0.0811 \left(\frac{r_0}{D}\right) \left(\frac{v(h)}{r_0}\right) \tag{6}$$

Given closed loop the centroid values (from telemetry) the residual tip/tilt across the full aperture can be easily calculated. Figures 2 and 3 are plots of open and closed tip/tilt loop PSDs. From these we estimate a 3dB break point of the AO tip/tilt correction to be approximately 5Hz. The root-mean-squared (RMS) wavefront error from tip/tilt can also be calculated directly from the RMS of the tip/tilt centroid values (σ_{ttcent} [rad]) across the whole aperture.

$$\sigma_{RT} = \sigma_{ttcent} \left(\frac{D}{4}\right) [m] \tag{7}$$

Where D is the diameter of the aperture, 5 meters in our case.

In our observations σ_{ttcent} was 0.0072 arcseconds, which results in σ_{RT} of 44 nm. The theoretical value using Eqs. 5,6,$r_0(0.5\ \mu m)$ = 10 cm, and f_3dB = 5Hz is 51 nm. The theoretical and measured values agree to within 15% and show that under the above seeing conditions the contribution from tip/tilt error is small.

2.3. Atmospheric Fitting Error σ^2_{AF}

The atmospheric fitting error made by a continuous face sheet DM is given by[8]:

$$\sigma^2_{AF} = 0.28 \left(\frac{d_s}{r_0}\right)^{5/3} [rad^2] \tag{8}$$

were r_0 is in meters at the wavelength of interest and d_s is the spacing between actuators in the pupil plane (31.2 cm for PALAO). For an $r_0(0.5\mu m)$ of 10 cm this results in σ_{AF} = 109 nm.

2.4. Telescope Fitting Error σ^2_{TF}

There is also a fitting error term for errors in the optics with spatial frequency greater then the actuator spacing of the DM, we call this σ^2_{TF}. Any errors in the AO optics that can not be corrected with the DM will be included as part of the calibration error term (see section 2.5). So, only optics that are not measured as part of the calibration procedure will contribute to σ^2_{TF}. The optics in question are then the telescope secondary, primary and one fold flat mirror that is used in the calibration procedure to fold the white light into the beam. Any fitting error from the 2 inch fold flat mirror would only serve to artificially increase the σ^2_{CAL} term.

The telescope primary and secondary high spatial frequency errors can be estimated from curvature sensing data collected in April 1995. We estimate that the DM can remove perfectly the first 25 Zernike terms. The curvature data predicts an RMS wavefront error of 100 nm after removal of the first 25 Zernike terms.

Table 1. On-axis Bright Guide Star Performance

Error term	RMS Wavefront Error $[nm]$	Mean-squared Wavefront Error $[nm^2]$
σ_{TD}	107	11449
σ_{RT}	51	2601
σ_{AF}	109	11881
σ_{TF}	100	10000
σ_{CAL}	165	27225
σ_{BGS}	251	63156

2.5. Calibration of desired centroid values σ^2_{CAL}

In general due to non-common path errors a perfect wavefront at a WFS is not a perfect wavefront on the science detector. One must determine what wavefront at the WFS creates a perfect (or near perfect) wavefront at the science image. We call this process image sharpening and the associated wavefront error from this σ_{CAL}.

The current process for image sharpening involves locking the AO system on a white light source and looking at the image formed on PHARO. Then different amounts of Zernike aberrations are added to the desired closed loop centroids values, a new PHARO image is taken and the affects of these aberrations on the closed loop image on PHARO is then evaluated by "eye" to determine if the image has been improved. The first 10 Zernike terms are determined by this iterative method. This procedure takes between 15 and 30 minutes.

In general this image sharpening procedure is carried out the first afternoon of every observing run (that is just after the AO system is mounted on the telescope) and then whenever there is a large ($\tilde{>}4^0C$) change in night time air/dome temperature. In addition we currently only perform the procedure on one or at most two filters, but in general the image should to be sharped and the new desired centroid offsets calculated for every PHARO filter (there are 12 of them) and each of the two plate scales (25 mas/pixel and 40 mas/pixel). The current method of image sharpening is to labor intensive, time consuming and (as will become apparent latter) is too inaccurate. We are currently looking into using phase diversity or phase retrieval techniques to automate and improve the image sharpening procedure.

On September, 27 1999, the above image sharpening procedure was carried out and K band images collected. The Strehl was evaluated using a package developed by Marshal, et al.[9] The K band images were diffraction limited in FWHM and had an estimated RMS wavefront error of 165 nm.

3. CONCLUSIONS AND LESSONS LEARNED

Table 1 show a summary of error terms in RMS wavefront and mean-squared wavefront. The total predicted RMS wavefront error is 251 nm. Under these atmospheric conditions we have achieved K band Strehls of 50% or (291 nm of wavefront error) and J band Strehls of 0.11 (284 nm of wavefront). This implies that the above analysis is not accounting for 149 nm in K or 135 nm at J of wavefront error.

The dominant error term is that from calibration (or image sharpening). As mentioned earlier we are currently looking into using phase-diversity or phase-retrieval techniques to automate and improve this procedure. We would expect such techniques to reduce σ_{CAL} to values less then 50 nm. The next largest terms (all of about equal size) are: σ_{TD}, σ_{AT}, and σ_{TF}. The Time-delay term can be decreased by increasing the computer speed and improving the servo control algorithm. The fitting error from the atmospheric can only be reduced by using a DM with more actuators and thus smaller subapetures. A 1600 actuator DM design has been investigated, it would provide subapetures of 12.5 cm and for $r_0(0.5\mu m)$= 10 cm a σ_{AT} of 51 nm. This upgrade would also help reduce the fitting error to the telescope. It is difficult to estimate the how much the telescope fitting error would decrease because of uncertainty in the curvature sensing measurements, but the value would not be larger then 50 nm. With the previously mentioned upgrades (which are currently unfunded) it should be possible to reduce all of the error terms to 50 nm or less, resulting in an RMS wavefront of 112 nm or K band Strehls of 90%.

ACKNOWLEDGMENTS

This work is being performed at the Jet Propulsion Laboratory, California Institute of Technology, under a contract with the National Aeronautics Space Administration

REFERENCES

1. R. G. Dekany, G. Brack, D. Palmer, B. R. Oppenheimer, T. L. Hayward, , and B. Brandl, "First tip-tilt correction with the Palomar 200-in adaptive optics system," in *Adaptive Optical System Technologies*, D. Bonnaccini and R. K. Tyson, eds., vol. 3353, pp. 56–59, SPIE, 1998.
2. R. G. Dekany, K. Wallace, G. Brack, B. R. Oppenheimer, and D. Palmer, "Initial test results from the Palomar 200" adaptive optics system," in *Adaptive Optics and Applications*, R. K. Tyson and R. Q. Fugate, eds., vol. 3126, pp. 269–276, SPIE, 1997.
3. J. H. Hardy, *Adaptive Optics for Astronomical Telescopes*, pp. 114–115. Oxford University Press, New York, 1st ed., 1998.
4. F. Dekens, *Atmospheric characterization for adaptive optics at the W. M. Keck and Hale Telescopes.* PhD thesis, University of California, Irvine, Jan. 1998.
5. J. H. Hardy, *Adaptive Optics for Astronomical Telescopes*, pp. 337–338. Oxford University Press, New York, 1st ed., 1998.
6. G. A. Tyer Report TR-887, The Optical Sciences Co., 1988.
7. G. Chanan, G. Djorgovski, A. Gleckler, S. Kulkarni, T. Mast, C. Max, J. Nelson, and P. Wizinowich, "*Adaptive Optics for Keck Observatory*," Keck Observatory Report No. 208, W.M. Keck Observatory, Kamuela HI, Jan. 1996.
8. J. H. Hardy, *Adaptive Optics for Astronomical Telescopes*, pp. 342–343. Oxford University Press, New York, 1st ed., 1998.
9. J. Marshall, M. Troy, and R. Dekany, "Anisoplanicity studies within NGC6871," in *Adaptive Optical System Technologies*, P. Wizinowich, ed., vol. 4007, SPIE, 2000.